

Temperature Range for Fiber-Form Nanostructure Growth on Molybdenum Surfaces due to Helium Plasma Irradiation

Shuichi TAKAMURA

Faculty of Engineering, Aichi Institute of Technology, Toyota 470-0392, Japan

(Received 1 May 2014 / Accepted 2 July 2014)

Nanostructure formation on molybdenum surfaces due to helium plasma exposure is investigated, with a focus on determining the temperature band for the growth of fiber-form nanostructures. Precise temperature measurements can be obtained using thin thermocouples inserted into sheet specimens. The temperature range for nanostructure growth was determined to be 800 ~ 1050 K under incident helium ion energies of 50 ~ 100 eV and an ion flux of $2 \times 10^{21} \text{ m}^{-2} \cdot \text{s}^{-1}$. Surface morphologies near the upper and lower boundary temperatures differ from those of a standard fiber-form nanostructure. In a standard case, nano-fibers of molybdenum were found to have diameters of approximately 50 nm, whereas those of tungsten are half of the molybdenum fibers.

© 2014 The Japan Society of Plasma Science and Nuclear Fusion Research

Keywords: fiber-form nanostructure, molybdenum, helium defect, surface temperature

DOI: 10.1585/pfr.9.1405131

1. Introduction

Since the discovery of fiber-form nanostructures caused by the helium plasma irradiation on tungsten surfaces [1, 2], many aspects have been investigated [3], with a focus on the formation mechanism of such nanostructures [4–6]. The physical mechanism is not clear so far although some modellings and MD (Molecular Dynamic) simulations have been tried. Therefore, studying similar structures on other refractory metal surfaces, such as molybdenum, is worthwhile. The formation of fiber-form nanostructures on molybdenum has been confirmed [7, 8], but not in detail.

Here, we focus on, first of all, the precise temperature range, over which fiber-form nanostructure formed on molybdenum surfaces. To exclude uncertainties in the spectral emissivity, we use thermocouples to measure the precise temperature range rather than radiation thermometers. Secondly, we study the surface morphology of molybdenum at the upper limit of the surface temperature in terms of the nanostructure formation and annihilation [9, 10]. Finally, differences nanostructures of tungsten and molybdenum are discussed.

2. Experimental Methods

To form nanostructures on molybdenum surfaces, we employed two kinds of helium plasma exposure techniques. The one shown in the insert of Fig. 1 (a), has no external cooling stage. The target with a thickness of 1 mm was suspended with an R-type thermocouple sleeve having a diameter of 0.5 mm; the thermocouple was inserted through the long hole parallel to the molybdenum surface. The formation of nanostructures can be confirmed by a de-

crease in the surface temperature due to the enhancement of black-body radiation from the target surface [9, 11], and by a visible recognition of black molybdenum surface, as shown in Fig. 1 (a).

Figure 1 (b-1) shows the schematic setup of the other method in which the reflected intensity of a green laser light with a wavelength of 532 nm is influenced by the surface morphology. The molybdenum sheet was placed on an indirectly cooled stage with a thin insulating mica sheet. A K-type thermocouple was inserted into the molybdenum sheet. The stage was attached to a copper rod on the vacuum side. The opposite end of the copper rod, on the atmospheric side, was cooled with the circulating cooling water, as shown in Fig. 1 (b-2).

Helium plasma exposures were performed in the AIT-PID (Aichi Institute of Technology – Plasma Irradiation Device), where high-density plasmas of more than $1.0 \times 10^{18} \text{ m}^{-3}$ are produced with a bulk electron temperature of 5 eV accompanied by energetic electrons whose apparent temperature is about 30 eV with a fraction of about 10% [12]. Before the helium plasma exposure, argon plasma was used to sputter surface contamination via biasing by -100 V for a few minutes.

3. Results and Discussion

3.1 Determination of temperature range

Figure 1 (a) shows a typical temporal evolution of nanostructure growth on a molybdenum surface without any external cooling. Just after the electrical biasing of the target (the ion incident energy was 80 eV), the temperature measured with the R-type thermocouple indicates 920 K. Then, the temperature gradually decreased associated with surface blackening and a reduction in the ion

author's e-mail: takamura@aitech.ac.jp

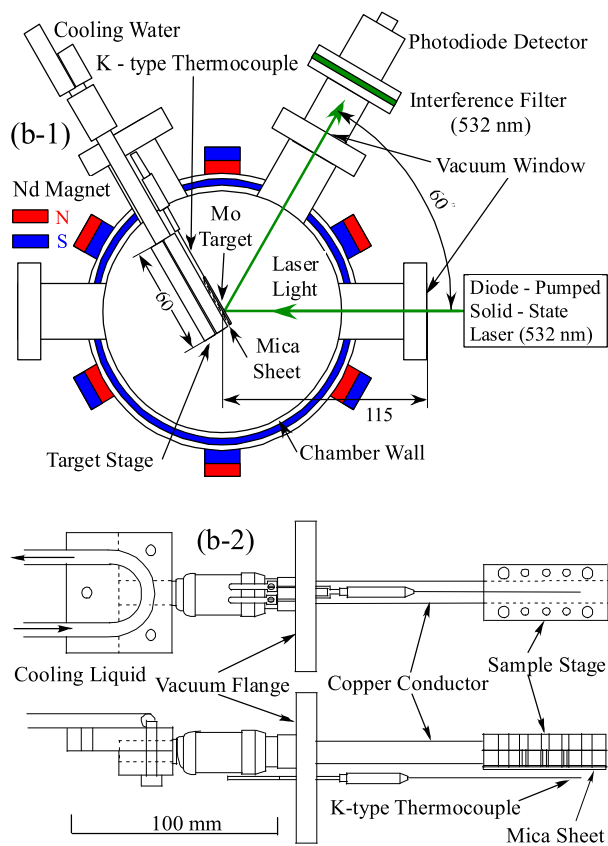
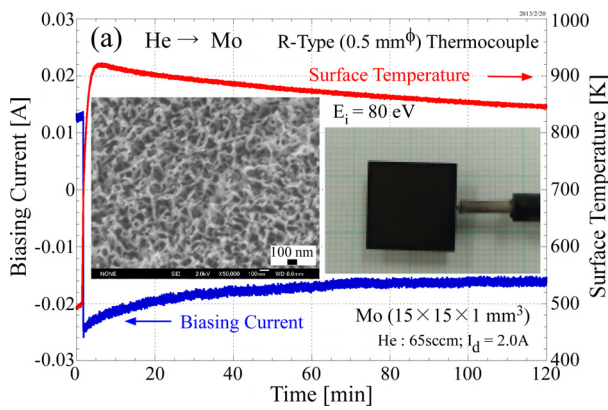


Fig. 1 Two methods for exposing molybdenum targets to helium plasmas: (a) Without a cooled stage, the target is suspended with an R-type thermocouple of 0.5 mm diameter in an insulated sleeve. (b) With the stage attached to a cooled copper rod of 95 mm diameter. (b-1) Laser light reflection due to a change in surface morphology, (b-2) Detail of sample stage with insulated mica sheet and K-type thermocouple.

saturation current due to the suppression of electron emissions [13]. The Scanning Electron Microscope (SEM) image shown in one of inserts to Fig. 1 (a) is very similar to that of nanostructured tungsten. Therefore, 920 K is well inside the temperature band for the growth of molybdenum nanostructures. Figure 2 shows other SEM photos of a cross section, obtained with the Cross-sectional Polishing (CP) method, using an argon ion beam.

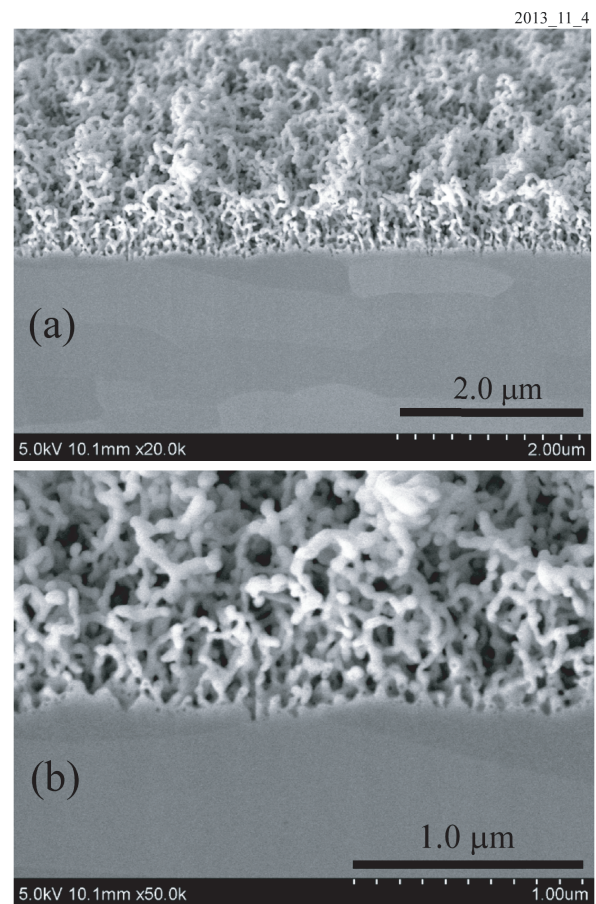


Fig. 2 Typical nanostructures on Mo surface in an oblique view on a cross-section obtained with the CP method. Ion energy $E_i \sim 100$ eV, $T \sim 1000$ K, ion flux $\Gamma_i \sim 1.2 \times 10^{21} \text{ m}^{-2} \cdot \text{s}^{-1}$, and fluence $\sim 8.6 \times 10^{24} \text{ m}^{-2}$.

A technique similar to that used in Fig. 1 (a) with the thermocouple was employed to determine the highest temperature that allows nanostructure growth. The molybdenum temperature was elevated up to approximately 1200 K and then reduced by decreasing the discharge current for plasma production at 10 min interval, as shown in Fig. 3. During each 10 min interval, the plasma condition was maintained constant, and simultaneously any temperature changes were examined. Even a slight decrease in temperature indicates the development of a nanostructure formation since any increase in total emissivity caused by nanostructure growth cools the molybdenum material due to an increase in black-body radiation. When the temperature was kept at 1065 K for two hours, we obtained neither reduction in molybdenum temperature nor blackening of its surface. From the above series of experiments, we conclude that the highest temperature would be 1050 K. Another observation was obtained in the scheme of the molybdenum placed on the indirectly cooled sample stage, as shown in Fig. 4, where the light reflection intensity decreased down to 6.7% of the starting reflected light intensity at 1045 K. A similar reduction was obtained at $T \sim 1050$ K, but a very small reduction was found at

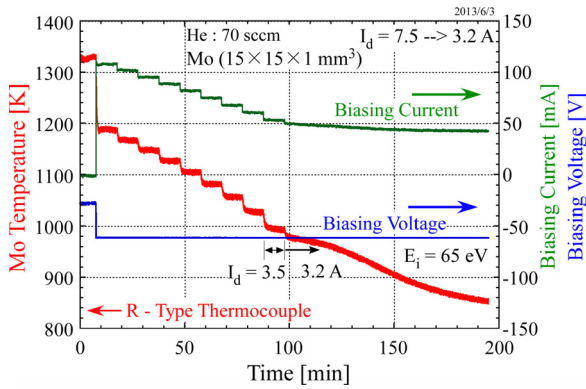


Fig. 3 Determination of upper temperature limit for nanostructure formation by discriminating a self-cooling of target. Exposure method was the same as that in Fig. 1 (a). The surface temperature was controlled by adjusting the discharge current. $\Gamma_i \sim 1.8 \times 10^{21} \text{ m}^{-2} \cdot \text{s}^{-1}$ at $T \sim 1050 \text{ K}$.

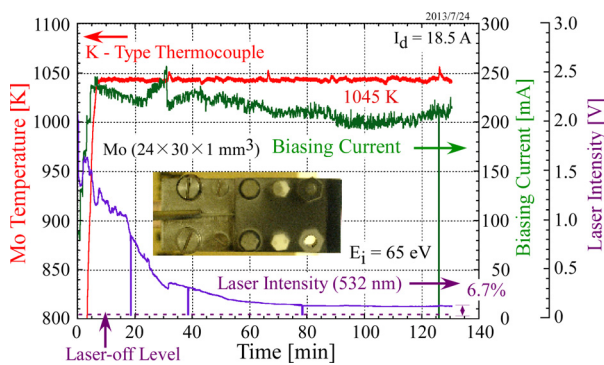


Fig. 4 Determination of upper temperature limit for nanostructure formation by a change in laser light reflection. The final laser light reflection intensity was about 6.7% of original one.

$T \sim 1060 \text{ K}$.

Figure 1 shows the nanostructure formation at $T \sim 920 \text{ K}$, the laser light reflection method shows the formation at $T \sim 870 \text{ K}$. Thus, as shown in Fig. 5 (a), we attempted the experiment at a temperature of 770 K . At this temperature laser light reflection did not decrease nor did the blackening of the plasma-facing surface occur so that 770 K should be too low to support the growth of the nanostructure. An increase in the surface temperature up to 830 K indicated a complete suppression of laser light reflection, as shown in Fig. 5 (b); therefore 830 K is very close to the lowest temperature for the nanostructure formation.

3.2 Surface morphology

Near the highest temperature for nanostructure growth, the surface morphology is somewhat different from the standard fiber-form nanostructure shown in Fig. 1 (a). Figure 6 shows two examples: (a) at 1045 K and (b) at 1055 K . In this temperature range, the fiber-

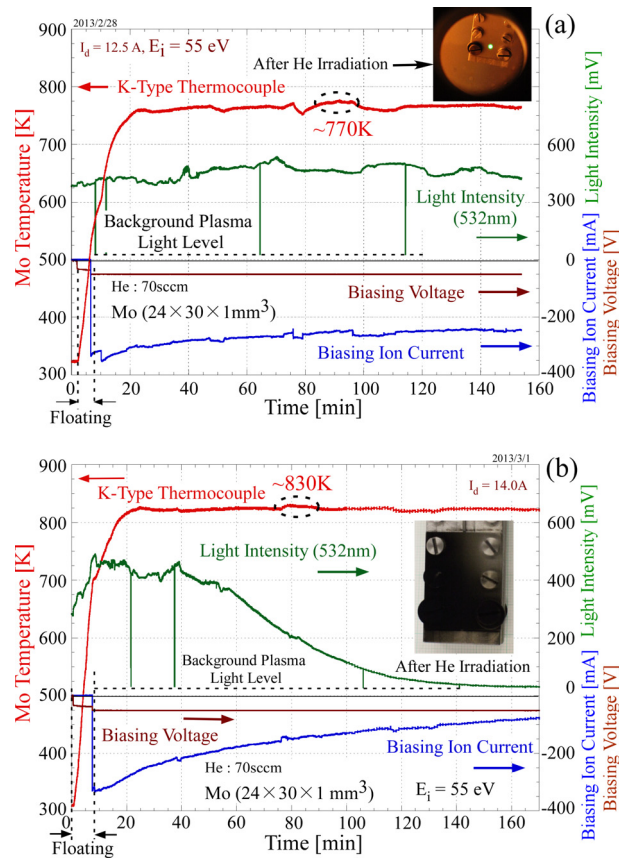


Fig. 5 Determination of lower temperature limit for nanostructure formation by a reduction in intensity of reflected laser light: (a) $T \sim 770 \text{ K}$, $\Gamma_i \sim 2.4 \times 10^{21} \text{ m}^{-2} \cdot \text{s}^{-1}$, fluence $\sim 2.2 \times 10^{25} \text{ m}^{-2}$ with $E_i \sim 55 \text{ eV}$; (b) $T \sim 830 \text{ K}$, $\Gamma_i \sim 2.4 \times 10^{21} \text{ m}^{-2} \cdot \text{s}^{-1}$, fluence $\sim 2.3 \times 10^{25} \text{ m}^{-2}$ with $E_i \sim 55 \text{ eV}$.

form nanostructure formation and its plasma annealing of the structure [8, 9] would proceed simultaneously. A detailed examination of Fig. 6 (a) reveals some traces of recovery caused by plasma annealing. Figure 6 (b) shows the enhancement of the recovery process. It is noted that the morphological change is very sensitive to even a small difference in the surface temperature near the high temperature limit. It seems that the nanostructure formation would be influenced by the viscosity of the corresponding refractory metals [5]. The viscosity would have similar temperature sensitivity, and the critical temperature would depend on the ion flux density.

Figure 7 compares the nanostructures for tungsten and molybdenum. The diameters of the nano-fibers of molybdenum are roughly twice those of tungsten.

4. Conclusions

A precise determination of the temperature band for the formation of fiber-form nanostructures has been performed, using thermocouples rather than radiation thermometers. Measurements with radiation thermometers can

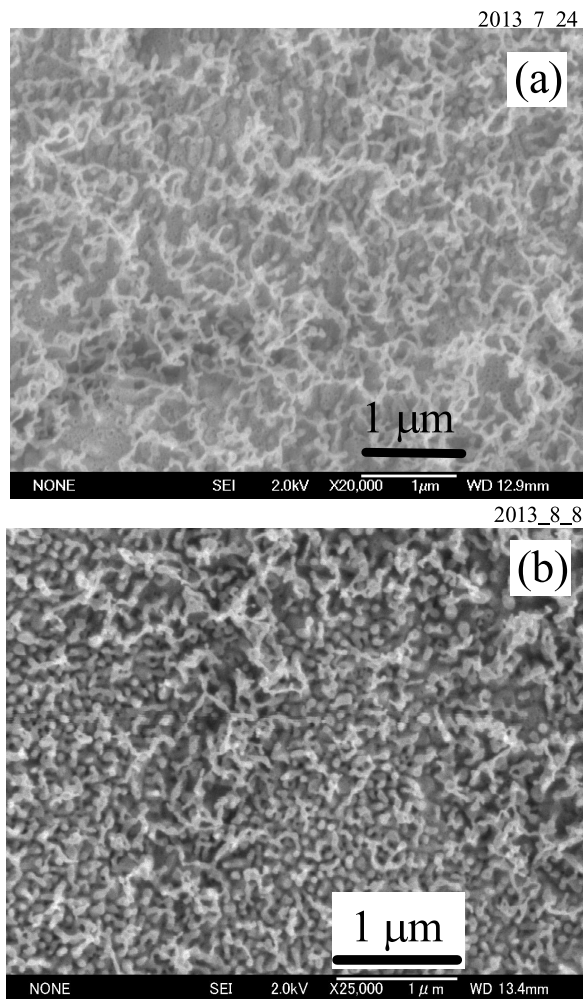


Fig. 6 Surface morphologies of He-defected molybdenum near the upper temperature limit; (a) $T \sim 1045$ K and (b) $T \sim 1055$ K. For (a), $\Gamma_i \sim 1.9 \times 10^{21} \text{ m}^{-2} \cdot \text{s}^{-1}$, fluence $\sim 1.4 \times 10^{25} \text{ m}^{-2}$ at $E_i \sim 65$ eV, and (b) $\Gamma_i \sim 2.3 \times 10^{21} \text{ m}^{-2} \cdot \text{s}^{-1}$, fluence $\sim 1.2 \times 10^{25} \text{ m}^{-2}$ at $E_i = 125 \sim 145$ eV.

have larger uncertainties due to ambiguities in the spectral emissivity of the molybdenum surface. Under incident ion energies of 50 ~ 100 eV, the maximum temperature for nanostructure growth is approximately 1050 K and the minimum is around 800 K. At the upper boundary temperature, nano-fiber growth competes with shrinkage due to plasma annealing. At the lower boundary temperature, the speed of growth is very low. Although the temperature band for nanostructure growth of molybdenum is located just below that for tungsten, the phenomena are very similar. But the thicknesses of nano-fibers on molybdenum are larger than those on tungsten.

Acknowledgment

The research work was supported by a Grant-in-Aid for Challenging Exploratory Research 23656578 and a Grant-in-Aid for Scientific Research 26420855 from JSPS. The author would like to thank the students in the plasma laboratory of AIT for their assistance, and Prof. N. Ohno,

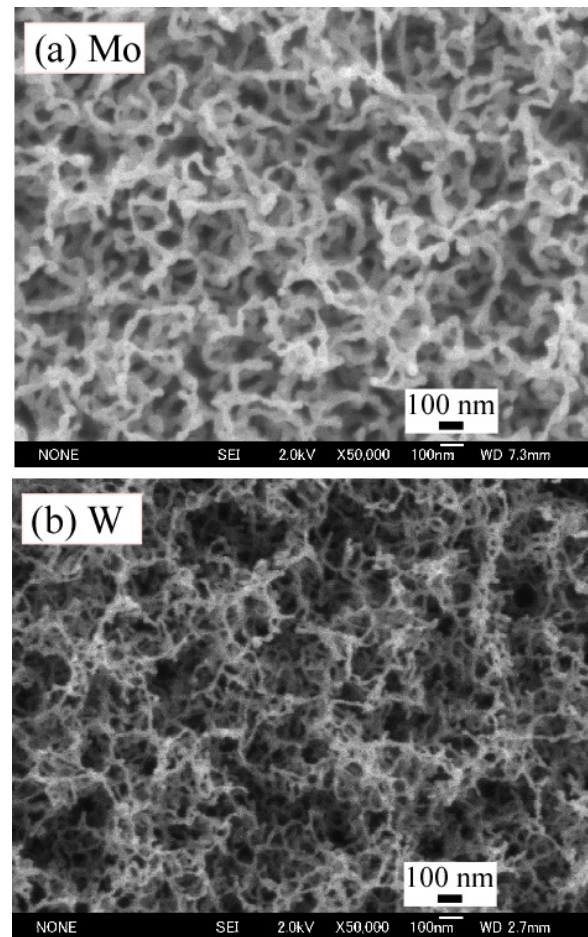


Fig. 7 Comparison of nano-fibers for (a) molybdenum and (b) tungsten.

Dr. S. Kajita, and Prof. Y. Uesugi for their discussions.

- [1] S. Takamura, N. Ohno, D. Nishijima and S. Kajita, *Plasma Fusion Res.* **1**, 051 (2006).
- [2] M.J. Baldwin and D.P. Doerner, *Nucl. Fusion* **48**, 035001 (2008).
- [3] S. Takamura, S. Kajita and N. Ohno, *BUTSURI* (Membership Journal of The Physical Society of Japan) **68**, 602 (2013) (in Japanese).
- [4] S.I. Krasheninnikov, *Phys. Scr.* **T145**, 014040 (2011).
- [5] R.D. Smirnov and S.I. Krasheninnikov, *Nucl. Fusion* **53**, 082002 (2013).
- [6] S. Takamura, *Plasma Fusion Res.* **9**, 1302007 (2014).
- [7] S. Kajita, W. Sakaguchi, N. Ohno, N. Yoshida and T. Saeki, *Nucl. Fusion* **49**, 09005 (2011).
- [8] S. Kajita, T. Saeki, Y. Hirahata and N. Ohno, *Jpn. J. Appl. Phys.* **50**, 01AH02 (2011).
- [9] S. Takamura, T. Miyamoto, Y. Tomida, T. Minagawa and N. Ohno, *J. Nucl. Mater.* **415**, S100 (2011).
- [10] T. Miyamoto, S. Takamura and H. Kurishita, *Plasma Sci. Technol.* **15**, 161 (2013).
- [11] S. Takamura, T. Miyamoto and N. Ohno, *J. Nucl. Mater.* **438**, S814 (2013).
- [12] S. Takamura, *IEEEJ Trans.* **7** (S1), S19 (2012).
- [13] S. Takamura, T. Miyamoto and N. Ohno, *Nucl. Fusion* **52**, 123001 (2012).